Equilibrium orbit analysis in a free-electron laser with a coaxial wiggler

B. Maraghechi,[1,2] B. Farrokhi,[1] J. E. Willett,[3] and U.-H. Hwang[4]
[1]*Institute for Studies in Theoretical Physics and Mathematics, P.O. Box 19395-5531, Tehran, Iran*
[2]*Department of Physics, Amir Kabir University, Tehran, Iran*
[3]*Department of Physics and Astronomy, University of Missouri–Columbia, Columbia, Missouri 65211*
[4]*Physics Department, Korea University of Technology and Education, Chunan, Choongnam 330-860, Korea*
(Received 29 July 1999)

An analysis of single-electron orbits in combined coaxial wiggler and axial guide magnetic fields is presented. Solutions of the equations of motion are developed in a form convenient for computing orbital velocity components and trajectories in the radially dependent wiggler. Simple analytical solutions are obtained in the radially-uniform-wiggler approximation and a formula for the derivative of the axial velocity $v_\parallel$ with respect to the Lorentz factor γ is derived. Results of numerical computations are presented and the characteristics of the equilibrium orbits are discussed. The third spatial harmonic of the coaxial wiggler field gives rise to group III orbits which are characterized by a strong negative mass regime.

PACS number(s): 41.60.Cr, 52.75.Ms

I. INTRODUCTION

Most free-electron lasers employ a wiggler with either a helically symmetric magnetic field generated by bifilar current windings or a linearly symmetric magnetic field generated by alternating stacks of permanent magnets. A uniform static guide magnetic field is also frequently employed. Single-particle orbits in these helical and planar fields combined with an axial guide field have been analyzed in detail and have played a role in the development of free-electron lasers [1]. The harmonics of gyroresonance for off-axis electrons caused by the radial variation of the magnetic field of a helical wiggler have been found by Chu and Lin [2]. Recently, the feasibility of using a coaxial wiggler in a free-electron laser has been investigated. Freund *et al.* [3,4] studied the performance of a coaxial hybrid iron wiggler consisting of a central rod and a coaxial ring of alternating ferrite and dielectric spacers inserted in a uniform static axial magnetic field. McDermott *et al.* [5] proposed the use of a wiggler consisting of a coaxial periodic permanent magnet and transmission line. Coaxial devices offer the possibility of generating higher power than conventional free-electron lasers and with a reduction in the beam energy required to generate radiation of a given wavelength.

In the present paper, single-particle orbits in a coaxial wiggler are studied. The wiggler magnetic field is radially dependent with the fundamental plus the third spatial harmonic component and a uniform static axial magnetic field present. In Sec. II the scalar equations of motion are introduced and reduced to a form that is correct to first order in the wiggler field. In Sec. III solutions of the equations of motion are developed in a form suitable for computing the electron orbital velocity and trajectory in the radially dependent magnetic field of a coaxial wiggler. The special case of a radially independent wiggler is also analyzed. In Sec. IV the results of numerical computations of the wiggler field components, velocity components, radial excursions, and the Φ function for locating negative mass regimes are presented and discussed. In Sec. V some conclusions are presented.

II. EQUATIONS OF MOTION

Electron motions in a static magnetic field **B** may be determined by solution of the vector equation of motion

$$\frac{d\mathbf{v}}{dt}=\frac{-e}{\gamma mc}\mathbf{v}\times\mathbf{B}, \tag{1}$$

where $\mathbf{v}, -e$, and m are the velocity, charge, and (rest) mass, respectively, of the electron. The Lorentz factor γ is a constant given by

$$\gamma=(1-v^2/c^2)^{-1/2}, \tag{2}$$

where $v=|\mathbf{v}|$ is the constant electron speed.

The total magnetic field inside a coaxial wiggler will be taken to be of the form

$$\mathbf{B}=B_r\hat{\mathbf{r}}+B_z\hat{\mathbf{z}}, \tag{3}$$

$$B_r=B_wF_r(r,z), \tag{4}$$

$$B_z=B_0+B_wF_z(r,z), \tag{5}$$

where B_0 is a uniform static axial guide field, and F_r and F_z are known functions of cylindrical coordinates r and z. Equation (1) may be written in the scalar form

$$\frac{dv_r}{dt}-\frac{v_\theta^2}{r}=-v_\theta(\Omega_0+\Omega_wF_z), \tag{6}$$

$$\frac{dv_\theta}{dt}+\frac{v_\theta v_r}{r}=v_r(\Omega_0+\Omega_wF_z)-v_z\Omega_wF_r, \tag{7}$$

$$\frac{dv_z}{dt}=v_\theta\Omega_wF_r; \tag{8}$$

Ω_0 and Ω_w are relativistic cyclotron frequencies given by

$$\Omega_0=\frac{eB_0}{\gamma mc}, \tag{9}$$

$$\Omega_w = \frac{eB_w}{\gamma mc}. \tag{10}$$

Initial conditions will be chosen such that the transverse motion of the electron in the B_0 field vanishes in the limit as B_w approaches zero. Then, in order to develop a solution to first order in the wiggler field B_w, the scalar equations of motion will be approximated by

$$\frac{dv_r}{dt} = -\Omega_0 v_\theta, \tag{11}$$

$$\frac{dv_\theta}{dt} = \Omega_0 v_r - v_\parallel \Omega_w F_r, \tag{12}$$

$$\frac{dv_z}{dt} = 0, \tag{13}$$

with the wiggler field approximated by the fundamental plus the third spatial harmonic component,

$$F_r = F_{r1}\sin(k_w z) + F_{r3}\sin(3k_w z), \tag{14}$$

where

$$F_{rn} \equiv G_n^{-1}[S_n I_1(nk_w r) + T_n K_1(nk_w r)], \tag{15}$$

$$G_n \equiv I_0(nk_w R_{out})K_0(nk_w R_{in}) - I_0(nk_w R_{in})K_0(nk_w R_{out}), \tag{16}$$

$$S_n \equiv \frac{2}{n\pi}\sin\left(\frac{n\pi}{2}\right)[K_0(nk_w R_{in}) + K_0(nk_w R_{out})], \tag{17}$$

$$T_n \equiv \frac{2}{n\pi}\sin\left(\frac{n\pi}{2}\right)[I_0(nk_w R_{in}) + I_0(nk_w R_{out})], \tag{18}$$

and $n = 1,3$; R_{in} and R_{out} are the inner and outer radii of the coaxial waveguide, $k_w = 2\pi/\lambda_w$ where λ_w is the wiggler (spatial) period, and I_0, I_1, K_0, and K_1 are modified Bessel functions.

III. ORBITAL ANALYSIS

A. Radially dependent wiggler

The scalar equations of motion may be solved to determine the electron orbital velocity and trajectory in a coaxial wiggler. Equation (13) yields

$$v_z = v_\parallel \tag{19}$$

where the constant $v_\parallel$ is the root-mean-square axial velocity component. With the initial axial position taken to be $z_0 = 0$,

$$z = v_\parallel t. \tag{20}$$

Equations (11), (12), (14), and (20) may be combined to obtain

$$\frac{d^2 v_r}{dt^2} + \Omega_0^2 v_r = f(t), \tag{21}$$

where

$$f(t) = \Omega_0 \Omega_w v_\parallel [F_{r1}\sin(k_w v_\parallel t) + F_{r3}\sin(3k_w v_\parallel t)]. \tag{22}$$

By the method of variation of parameters, a solution of Eq. (21) may be obtained in the form

$$v_r = \left(-v_{\theta 0} + \Omega_0^{-1}\int_0^t f(\tau)\cos(\Omega_0\tau)\,d\tau\right)\sin(\Omega_0 t) + \left(v_{r0} - \Omega_0^{-1}\int_0^t f(\tau)\sin(\Omega_0\tau)\,d\tau\right)\cos(\Omega_0 t), \tag{23}$$

where v_{r0} and $v_{\theta 0}$ are the initial radial and azimuthal velocity components. Then Eq. (11) yields

$$v_\theta = \left(v_{\theta 0} - \Omega_0^{-1}\int_0^t f(\tau)\cos(\Omega_0\tau)\,d\tau\right)\cos(\Omega_0 t) + \left(v_{r0} - \Omega_0^{-1}\int_0^t f(\tau)\sin(\Omega_0\tau)\,d\tau\right)\sin(\Omega_0 t). \tag{24}$$

The orbital velocity is given to first order in B_w by Eqs. (23), (24), and (19). The trajectory may then be computed using

$$r = r_0 + \int_0^t v_r(\tau)\,d\tau, \tag{25}$$

$$\theta = \theta_0 + \int_0^t v_\theta(\tau)\,d\tau, \tag{26}$$

and Eq. (20).

B. Radially uniform wiggler

By neglecting the radial variation of F_{r1} and F_{r3}, a solution of Eq. (21) may be obtained in the form

$$v_r = \alpha_1\sin(k_w v_\parallel t) + \alpha_3\sin(3k_w v_\parallel t), \tag{27}$$

where

$$\alpha_n = \frac{\Omega_0 \Omega_w v_\parallel F_{rn}}{\Omega_0^2 - n^2 k_w^2 v_\parallel^2} \quad (n = 1,3). \tag{28}$$

Equation (11) then yields

$$v_\theta = -\Omega_0^{-1} k_w v_\parallel \alpha_1 \cos(k_w v_\parallel t) - \Omega_0^{-1}(3k_w v_\parallel \alpha_3)\cos(3k_w v_\parallel t). \tag{29}$$

The corresponding initial conditions are

$$v_{r0} = 0, \tag{30}$$

$$v_{\theta 0} = -\Omega_0^{-1} k_w v_\parallel \alpha_1 - \Omega_0^{-1}(3k_w v_\parallel \alpha_3). \tag{31}$$

Root-mean-square values of the velocity components may be determined by use of Eqs. (27), (28), and (19). Replacing v^2 by its root-mean-square value in Eq. (2) then yields

$$\frac{v_\parallel^2}{c^2}\left[1+\frac{1}{2}\left(\frac{\alpha_1}{v_\parallel}\right)^2+\frac{1}{2}\Omega_0^{-2}k_w^2\alpha_1^2+\frac{1}{2}\left(\frac{\alpha_3}{v_\parallel}\right)^2+\frac{9}{2}\Omega_0^{-2}k_w^2\alpha_3^2\right]=1-\gamma^{-2}. \tag{32}$$

The derivative of $v_\parallel$ with respect to γ may be obtained from Eq. (32) and, after some algebra, cast into the form

$$\frac{dv_\parallel}{d\gamma}=\frac{c^2}{\gamma\gamma_\parallel^2 v_\parallel}\Phi, \tag{33}$$

where

$$\Phi=1-\frac{\sum_{n=1,3}(\Omega_0^2-n^2k_w^2v_\parallel^2)^{-3}\gamma_\parallel^2\Omega_w^2F_{rn}^2\Omega_0^2(\Omega_0^2+3n^2k_w^2v_\parallel^2)}{2+\sum_{n=1,3}(\Omega_0^2-n^2k_w^2v_\parallel^2)^{-3}\Omega_w^2F_{rn}^2\Omega_0^2(\Omega_0^2+3n^2k_w^2v_\parallel^2)}. \tag{34}$$

This equation may be used to establish the existence of a negative mass regime.

IV. NUMERICAL RESULTS

A numerical computation was conducted to investigate the properties of the equilibrium orbits of electrons inside a coaxial wiggler. The wiggler wavelength $2\pi/k_w$ and laboratory-frame electron density n_0 were taken to be 3 cm and 10^{12} cm^{-3}, respectively. The wiggler magnetic field B_w was taken to be 3745 G, which corresponds to the relativistic wiggler frequency $\Omega_w/ck_w=0.442$. The electron-beam energy $(\gamma-1)m_0c^2$ was taken to be 700 keV, corresponding to a Lorentz factor $\gamma=2.37$. The axial magnetic field B_0 was varied from 0 to 25.3 kG, corresponding to a variation from 0 to 3 in the normalized relativistic cyclotron frequency Ω_0/ck_w associated with B_0. The inner and outer radii of the coaxial wiggler were assumed to be $R_{in}=1.5$ cm and $R_{out}=3$ cm, respectively.

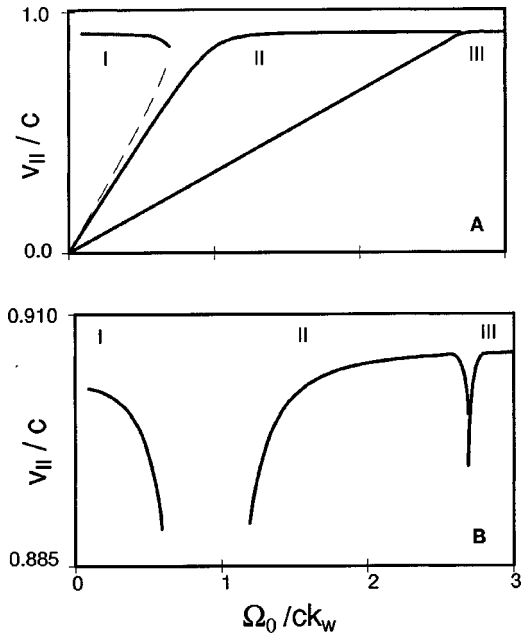

FIG. 1. Normalized axial velocity $v_\parallel/c$ as a function of the normalized axial guide magnetic field Ω_0/ck_w for group I, II, and III orbits. Narrow width of the second resonance at $\Omega_0/ck_w\approx2.7$ compared to the width of the first magnetoresonance at $\Omega_0\approx k_wv_\parallel$ is illustrated in Fig. 1(b).

Figure 1 shows the variation of the axial velocity of the quasi-steady-state orbits with the axial guide magnetic field for three classes of solutions, group I orbits for which $0<\Omega_0<k_wv_\parallel$, group II orbits with $k_wv_\parallel<\Omega_0<3k_wv_\parallel$, and group III orbits with $\Omega_0>3k_wv_\parallel$. The existence of group III orbits is due to the presence of the third spatial harmonic of the wiggler field, which also produces the second magnetoresonance at $\Omega_0\approx3k_wv_\parallel$. The narrow width of the second resonance at $\Omega_0/ck_w\approx2.7$ compared to the width of the first magnetoresonance at $\Omega_0\approx k_wv_\parallel$ is illustrated in Fig. 1(b). This is due to the relatively weak third harmonic compared to the fundamental component of the wiggler field. It should be noted that, although the exact resonances $\Omega_0=k_wv_\parallel$ and $\Omega_0=3k_wv_\parallel$ occur at the origin where $v_\parallel/c=\Omega_0/ck_w=0$, the ''first magnetoresonance'' in the literature refers to the group II orbits with cyclotron frequencies around $\Omega_0/ck_w\approx1$ in Fig. 1. Similarly, we refer to the group III orbits with cyclotron frequency around $\Omega_0/ck_w\approx2.7$ as the second magnetoresonance.

The rate of change of the electron axial velocity with electron energy is proportional to Φ and is equal to unity in the absence of the wiggler field. Figure 2 illustrates the de-

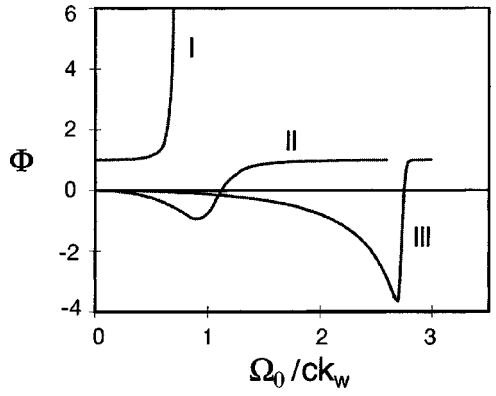

FIG. 2. Factor Φ as a function of the normalized axial guide magnetic field Ω_0/ck_w for group I, II, and III orbits.

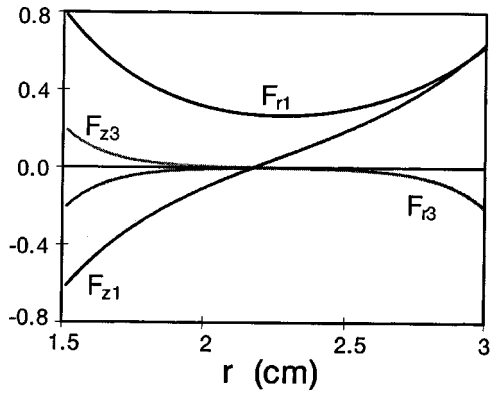

FIG. 3. Radial dependence of the radial and axial magnetic fields (divided by $B_w = 3745$ G) in the coaxial wiggler for the fundamental and third spatial harmonics.

pendence of Φ on the radial wiggler magnetic field and the axial guide magnetic field B_0. The curves corresponding to the group I and II orbits are almost unaffected by the third harmonic and are almost the same as in Ref. [6], where the third harmonic is neglected. A negative mass regime (i.e., negative Φ for which a decrease in the axial velocity results in an increase in the electron energy) is found for group III orbits that is stronger than that of the group II orbits.

Equations (15)–(18) are used to calculate the radial components of the wiggler field F_{r1} and F_{r3}. For the axial component the following expressions are used [4]:

$$F_z = F_{z1}\cos(k_w z) + F_{z3}\cos(3k_w z), \tag{35}$$

$$F_{zn} = G_n^{-1}[S_n I_0(nk_w r) - T_n K_0(nk_w r)]. \tag{36}$$

Figure 3 shows the variation of the amplitudes of the wiggler magnetic field (divided by $B_w = 3745$ G) with radius, for the first and third spatial harmonics. For the first harmonic the radial component F_{r1} has a minimum at $r \approx 2.28$ cm and the axial component F_{z1} changes sign around this point. McDermott *et al.* [5] have demonstrated the stability of a thin annular electron beam when F_{r1} is minimum at the beam radius. The radial and axial components of the third harmonic of the wiggler F_{r3} and F_{z3} are also shown in Fig. 3. The magnitudes of F_{r3} and F_{z3} are both minimum at $r \approx 2.28$ cm where F_{r1} is minimum. This is actually an inflection point for F_{z3}.

Variations of the radial components of the first and third spatial harmonics of the normalized wiggler magnetic field F_{r1} and F_{r3} with the wiggler wave number k_w are shown in Fig. 4. Figure 4 also shows the dimensionless transverse velocity coefficients $\bar{\alpha}_1 = \alpha_1/c$ and $\bar{\alpha}_3 = \alpha_3/c$ for the initial orbit radius $r_0 \approx 2.28$ cm where F_{r1} is minimum. The cyclotron frequency $\Omega_0/ck_w \approx 2.7$ is taken at the second magnetoresonance, and our choice of 3 cm for the wiggler wavelength corresponds to $k_w \approx 2.1$ cm^{-1}. It can be observed that at this wave number, although the radial component of the wiggler field at the first harmonic F_{r1} is much larger than at the third harmonic F_{r3}, the transverse velocity coefficients of the third harmonic $\bar{\alpha}_3$ are larger than $\bar{\alpha}_1$. This shows that the third harmonic may have considerable effect around the second magnetoresonance at $\Omega_0 \approx 3k_w v_\parallel$. Away from this resonance Eq. (28) shows that α_3 will be of the order of F_{r3}.

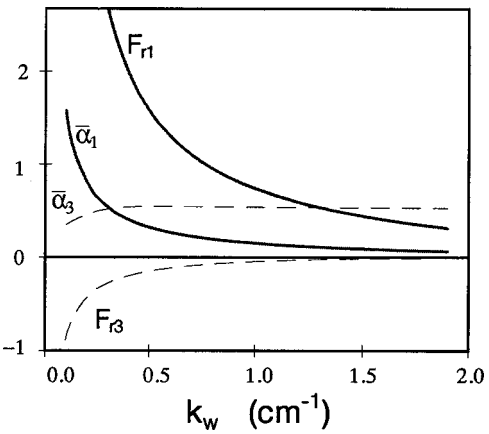

FIG. 4. Wave-number dependence of the radial components of the normalized wiggler magnetic field F_{r1}, F_{r3} and the dimensionless transverse velocity coefficients $\bar{\alpha}_1, \bar{\alpha}_3$. The normalized cyclotron frequency $\Omega_0/ck_w = 2.7$ is taken at the second magnetoresonance and $r_0 = 2.28$ cm.

In order to study the transverse motion of electrons in the radially dependent wiggler field, Eqs. (11), (12), (25), and (26) are solved numerically with the initial conditions chosen so that, in the limit of zero wiggler field, there is axial motion at constant velocity $v_\parallel$ but no Larmor motion. Figure 5 shows the variation of the radial and azimuthal components of electron velocity with $z(=v_\parallel t)$. The normalized cyclotron frequency Ω_0/ck_w is chosen to be 0.5, 1.2, and 3 for group I, II, and III orbits, respectively, which are somewhat away from the magnetoresonances. Solid curves correspond to the initial orbit radius $r_0 = 2.28$ cm, which is at the point where F_{r1} is minimum. Broken curves correspond to $r_0 = 1.8$ cm,

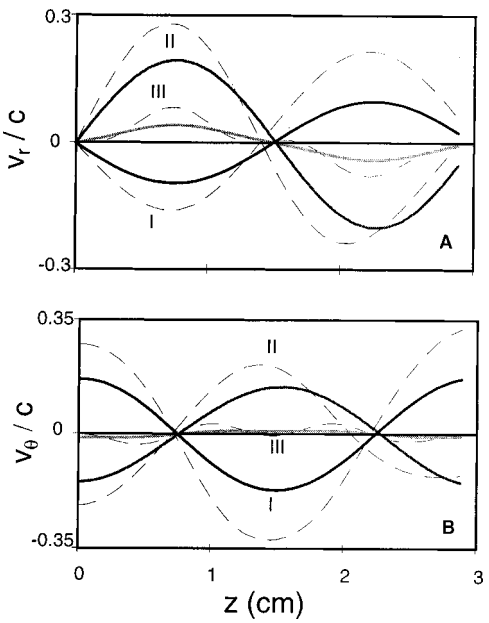

FIG. 5. Normalized transverse velocity components as a function of axial distance z for the initial orbit radius $r_0 = 2.28$ cm (solid curves) and $r_0 = 1.8$ cm (dashed curves). The normalized cyclotron frequency Ω_0/ck_w is 0.5, 1.2, and 3 for the group I, II, and III orbits, respectively.

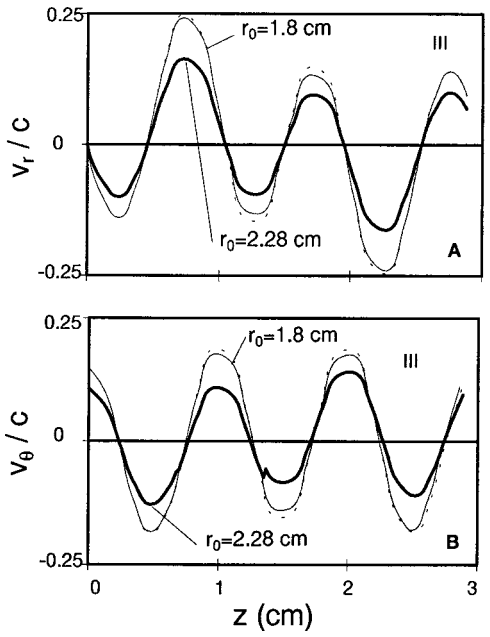

FIG. 6. Normalized transverse velocity components as a function of axial distance z for group III orbits, at the second magnetoresonance $\Omega_0/ck_w=2.7$. Solid curves correspond to the radially dependent wiggler and broken curves correspond to the radially independent wiggler.

which is away from the F_{r1} minimum. It can be observed that the spatial periodicity of v_r and v_θ for the first two groups is equal to one wiggler wavelength, which is the same as that of the first harmonic. Although group III orbits have a clear sinusoidal shape at $r_0=2.28$ cm (solid curves), slight deviations from sinusoidal shape are obvious at $r_0=1.8$ cm (broken curves). This is because at $r_0=2.28$ cm where F_{r1} is minimum F_{r3} is very small. Therefore away from the resonance the third harmonic plays almost no role (at $r_0=2.28$ cm). Moving away from the F_{r1} minimum to $r_0=1.8$ cm, however, increases the magnitude of F_{r3} slightly, making the effect of the third harmonic noticeable on group III orbits, which are away from the second magnetoresonance, in Fig. 5.

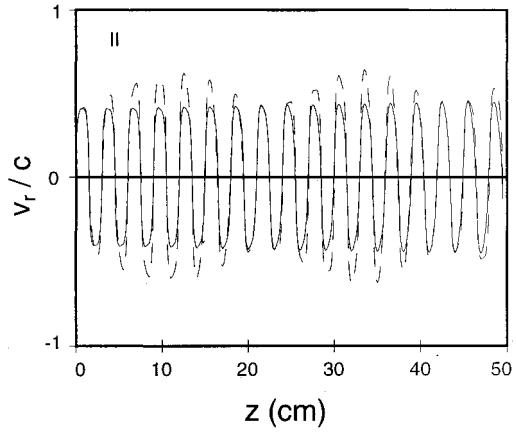

FIG. 7. Normalized radial velocity as a function of axial distance z for group II orbits at the first magnetoresonance $\Omega_0/ck_w=0.9$ with $r_0=2.28$ cm. Solid curves correspond to the radially dependent wiggler and broken curves correspond to the radially independent wiggler.

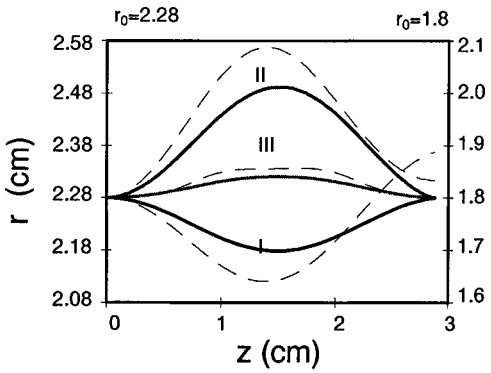

FIG. 8. Radial excursion r as a function of axial distance z for $r_0=2.28$ cm (solid curves) and $r_0=1.8$ cm (broken curves) for group I, II, and III orbits out of resonance at $\Omega_0/ck_w=0.5$, 1.2, and 3, respectively.

Figure 6 shows the variations of v_r/c and v_θ/c with z $(=v_\parallel t)$ for group III orbits when the cyclotron frequency is adjusted to the second magnetoresonance at $\Omega_0/ck_w\approx 2.7$. At $r_0=2.28$ cm the periodicity is approximately equal to $\lambda_w/3$, which is the same as that of the third harmonic, and shows the strong influence of the third harmonic on the transverse velocity components. Going away from the F_{r1} minimum to $r_0=1.8$ cm makes the amplitudes of oscillation of v_r and v_θ larger. Broken curves correspond to the solutions of Eqs. (27) and (29) when the radial variation of the wiggler field is neglected. These solutions do not differ appreciably from the r-dependent solutions for $r_0=2.28$ cm, because at minimum F_{r1} the radial excursions are small for group III orbits. Away from the F_{r1} minimum at $r_0=1.8$ cm, however, deviations are noticeable due to the larger radial excursions.

Figure 7 shows v_r/c versus z for group II orbits for the r-dependent wiggler (broken curves) and r-independent wiggler (solid curves). The initial orbit radius is taken at $r_0=2.28$ cm and the cyclotron frequency is chosen around the first magnetoresonance at $\Omega_0/ck_w=0.9$. Large radial excursions of electrons for group II orbits make the transverse velocity strongly affected by the radial dependency of the wiggler field. The amplitude is also modulated in space with a wavelength of around $16\lambda_w=48$ cm.

The radial excursion r shown in Fig. 8 corresponds to the cyclotron frequencies away from the magnetoresonances at

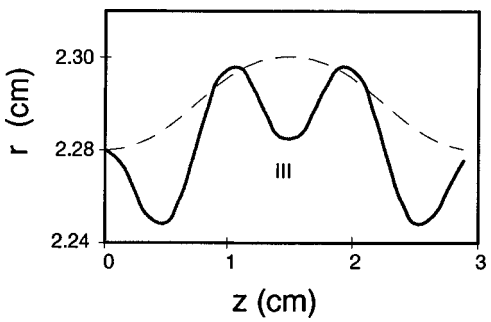

FIG. 9. Radial excursion r as a function of axial distance z for group III orbits at $r_0=2.28$ cm. Solid curve corresponds to resonance at $\Omega_0/ck_w=2.7$ and broken curve corresponds to out of resonance at $\Omega_0/ck_w=3$.

Ω_0/ck_w equal to 0.5, 1.2, and 3 for the group I, II, and III orbits, respectively. Solid curves correspond to the $r_0 = 2.28$ cm and the broken curves correspond to $r_0 = 1.8$ cm. It can be seen that when the electrons are injected into the wiggler at $r_0 = 2.28$ cm, where F_{r1} is minimum, the electron orbits remain well away from the waveguide walls at $R_{in} = 1.5$ cm and $R_{out} = 3$ cm.

Figure 9 compares the radial excursions of group III orbits at the second magnetoresonance at $\Omega_0/ck_w = 2.7$, (solid curve) with those slightly away from the resonance at $\Omega_0/ck_w = 3$ (broken curve). The influence of the third harmonic can be clearly seen through the modulation of the third harmonic by the first harmonic when the cyclotron frequency is adjusted at the second magnetoresonance.

V. CONCLUSIONS

The third spatial harmonic of the coaxial wiggler field gives rise to group III orbits with $\Omega_0 > 3k_w v_\parallel$. This relatively weak third harmonic makes the width of the second magnetoresonance narrow compared to the first magnetoresonance. A strong negative mass regime is found for the group III orbits. By adjusting the cyclotron frequency at the second magnetoresonance, the wiggler-induced velocity of the group III orbits was found to increase considerably. When the electrons are injected into the wiggler where its magnetic field is minimum, the electron orbits remain well away from the waveguide boundaries.

Harmonic gyroresonance of electrons in a combined helical wiggler and axial guide magnetic field has been reported by Chu and Lin [2]. In their analysis the relativistic single-particle equation of motion is used, with the axial velocity as well as the axial magnetic field of the wiggler averaged along the axial direction. By assuming near-steady-state orbits for off-axis electrons they found that the radial variation of the wiggler magnetic field produces a harmonic structure in the transverse force. This force, in turn, comprises oscillations at all harmonics of $k_w z$. It should be noted that there is no harmonic structure in the helical wiggler itself and the higher velocity harmonics vanish for the exact steady-state orbits of the on-axis electrons. Moreover, higher harmonics do not appear in the one-dimensional helical wiggler where the radial variation is neglected.

In the present analysis of a coaxial wiggler, on the other hand, the equation of motion is written to first order in the wiggler amplitude. With this approximation, the axial component of the wiggler field makes no contribution to the problem, leaving the axial velocity as a constant. The magnetic field of a coaxial wiggler is composed of a fundamental plus a large number of odd spatial harmonics, which appear directly in the magnetic force represented by $f(t)$ in Eq. (22). The third harmonic in $f(t)$ appears in the transverse velocity components as a part of the integrands in Eqs. (23) and (24) and is also demonstrated numerically for the radially dependent coaxial wiggler, but for the radially uniform wiggler the third harmonic is explicit in the solutions Eqs. (27)–(29).

[1] H. P. Freund and J. M. Antonsen, Jr., *Principles of Free-Electron Laser* (Chapman and Hall, London, 1996), Chap. 2.
[2] K. R. Chu and A. T. Lin, Phys. Rev. E **67**, 3235 (1991).
[3] H. P. Freund, R. H. Jackson, D. E. Pershing, and J. M. Taccetti, Phys. Plasmas **1**, 1046 (1994).
[4] H. P. Freund, M. E. Read, R. H. Jackson, D. E. Pershing, and J. M. Taccetti, Phys. Plasmas **2**, 1755 (1995).
[5] D. B. McDermott, A. J. Balkcum, R. M. Phillips, and N. C. Luhmann, Jr., Phys. Plasmas **2**, 4332 (1995).
[6] J. E. Willett, U. Hwang, Y. Aktas, and H. Mehdian, Phys. Rev. E **57**, 2262 (1998).